Mat. Res. Bull. Vol. 14, pp. 163-175, 1979. Printed in the USA. 0025-5408/79/020163-13$2.00/0

In_2O_3 : (Sn) AND SnO_2 : (F) FILMS - APPLICATION TO SOLAR ENERGY CONVERSION PART II - ELECTRICAL AND OPTICAL PROPERTIES

J.-C. Manifacier, L. Szepessy, J. F. Bresse, M. Perotin
Université des Sciences et Techniques du Languedoc
Centre d'Etudes d'Electronique des Solides (C.M.R.S. L.A. 21)
Place E. Bataillon, 34060 Montpellier Cedex

and

R. Stuck
Centre de Recherches Nucleaires
Groupe de Physique et Applications des Semiconducteurs Phase
23, rue du Loess, 67037 Strasbourg, France

(Received October 25, 1978; Refereed)

ABSTRACT

Highly conductive and transparent thin films of SnO_2 : F and In_2O_3 : Sn have been prepared using the simple pyrolitic (spray) method. The electrical properties of these layers are studied in relation to their dopant concentrations and their stoichiometric deviation. Typically we obtained for In_2O_3 : Sn and SnO_2 : F layers having the best overall properties (higher transparency and lower sheet resistance), resistivities ranging between 4 and 6.10^{-4} Ω cm with transparency exceeding 85% over the visible and near infra-red range of the spectrum. Emphasis is put on the possible applications of these films in solar energy conversion systems (solar cell and flat plate collectors technology).

Introduction

The conditions of preparation and characterization of these layers have been reported in the preceding paper (1). These layers are remarkable in that they are easily prepared in a very conductive form and have:

1. a high transparency across the visible and near infra-red (I.R.) spectrum, so they can be used as transparent and protective electrodes in the fabrication of solar cell structures (heterojunction or Schottky diodes). Moreover, due to their relatively low fabrication temperature (400 - 500°C), they could be used on polycrys-

talline silicon substrates in future technology.

2. a high reflectivity in the I.R.; the plasma frequency of carriers lies in the near infra-red region depending on the carrier density, so they can be used in flat plate collectors technology as spectral selective windows with large transmission for solar radiation and high reflection for thermal I.R. thus increasing the efficiency of the black-body collector.

Extraneous impurities have been introduced into the lattice: fluorine for SnO_2 and tin for In_2O_3 in order to increase the conductivity withour altering the transparency. We will report here the electrical and optical properties of these doped layers.

Electrical Properties

Hall measurements were carried out between 7K and 350K to determine the value of the carrier concentration n and the mobility μ_H. Thickness values were obtained from transmission measurements (see optical properties). The properties of a number of typical films with the lowest sheet resistance and highest optical transparency are listed in Table 1. The electrical conductivity is n-type, the best results have been obtained with In_2O_3 : Sn and SnO_2 : F layers. A free electron density of $n \sim 10^{21} cm^{-3}$ is achieved corresponding to a strongly degenerate semiconductor. Measurements have been made for samples having thicknesses over 0.15 μm; no dependence of the mobility on thickness was observed as it is sometimes reported for thinner layers (2).

TABLE 1

Physical properties of typical films.

	SnO_2 undoped	SnO_2 : F (NH_4F weight concentration in solution 1 = 1.3%)	In_2O_3 undoped	In_2O_3 : Sn ($SnCl_4\ 5H_2O$, weight concentration in solution 2 = 0.24%)
T_1 (°C)	560	560	560	560
T_2 (°C)	460	500	490	506
spraying time (min)	3	3	3	3
gas flow rate ($l.min^{-1}$)	3	3	3	3
$R_\square$ (Ω)	85	10.6	190	19
t (μm)	0.59	0.53	0.14	0.25
ρ (Ω.cm)	50.10^{-4}	$5.6\ 10^{-4}$	$27\ 10^{-4}$	$4.8\ 10^{-4}$
n (cm^{-3})	$9.5\ 10^{19}$	$1.05\ 10^{21}$	$7.8\ 10^{19}$	$8\ 10^{20}$
μ_H ($cm^2V^{-1}s^{-1}$)	13	10.6	30.1	16.1
Transmission (%)	80 - 90% (λ = 0.5 to 2 μm) Interference effects	85%(λ=0.5μm) 86%(λ=1.1 μm) 13%(λ=2μm)	80 - 95% (λ = 0.5 to 2 μm) Interference effects	85 - 95% (λ =0.4 to 1.5μm) 65%(λ=2μm)

SnO_2 samples:

For SnO_2 and SnO_2 : F samples, a weak dependence of the mobility on F concentration is noted (cf. Table 1); the variation of the resistivity is mainly due to a variation of carrier concentration. The value of resistivity and Hall coefficient $R_H = 1/ne$ (assuming that the Hall factor is equal to unity for our high conductivity samples) was found to be practically constant with temperature between 9K and 350K for doped samples: $n > 6 - 8.10^{19}$ cm^{-3}. For layers with lower carrier concentration, $n \sim 5 - 6.10^{19}$ cm^{-3}, a dependence of $\mu_H \sim T^{0.5-1}$ is observed versus temperature. For spray SnO_2, Van der Maesen and Witmer (2) observe a variation: $\mu_H \sim T^{1.16}$ between 100 and 300K, but the very weak variation of the carrier concentration versus temperature is not well enough established to deduce an activation energy.

In_2O_3 samples:

For the In_2O_3 : Sn samples, the values of the carrier concentration and the mobility are much more dependent on the dopant (tin) concentration than in the case of the SnO_2 : F layers. At ambient temperature, the values of n and μ_H versus tin concentration are reported in Figure 1. The Sn/In atomic ratio in the deposit deduced from the Sn/In atomic ratio in the solution (cf. Figure 3 of the preceding article (1)) is also indicated in Figure 1. A maximum is observed in the carrier concentration for a $SnCl_4$, $5H_2O$ weight concentration around 0.3%, corresponding to an atomic ratio Sn/In = 0.04 in the layer. For low Sn/In ratio, the increase in n corresponds to an increase in the tin concentration in the film. The decrease of n for a large addition of Sn is explained by a loss of crystallinity becoming progressively more pronounced as more tin is added, causing the electron density to decrease. (Impurities in the structure of amorphous semiconductors do not act as donors as they would in polycrystalline ones (3). At ambient temperature, the behavior of μ_H matches qualitatively with the supposition of carrier scattering due to the grain boundaries. Muller (4) in the case of In_2O_3 made by reactive sputtering observed a predominant scattering at ionized imperfection centers, and Goth (5), in the case of doped In_2O_3 made using a spray method, found that μ_H is strongly dependent on the impurity used, suggesting that car-

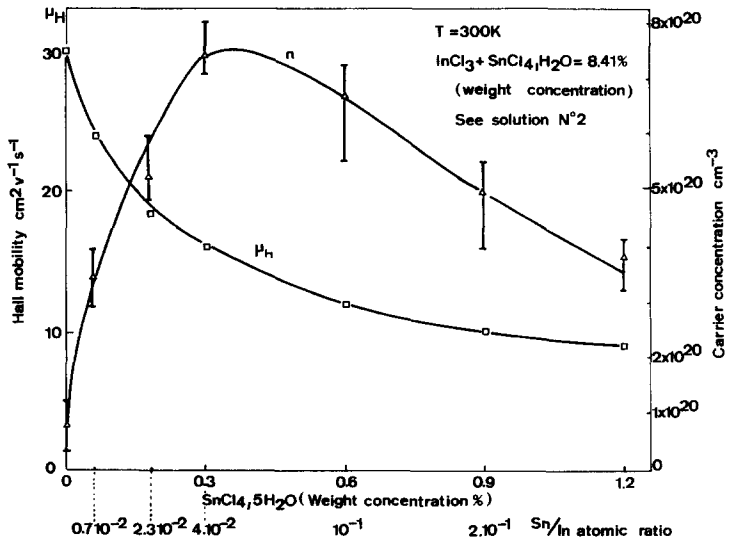

FIG. 1

Variation of the carrier concentration and Hall mobility versus tin concentration -- In_2O_3 : Sn layers.

rier scattering is mainly due to grain boundaries. In our layers, the concentration of these ionized imperfection centers increases continuously with the increase of the Sn/In atomic ratio, explaining the continuous decrease for μ_H (cf. Figure 1), while the density of ionized donors follows the same dependence as the carrier concentration.

As in the case of SnO_2 : F layers, the temperature dependence of μ_H and n for our highly doped ($n > 5.10^{19}$) In_2O_3 : Sn layers is very weak between 9 and 350K. This corresponds to the case of a highly degenerate electron gas (2, 4, 6) for which the mean velocity is nearly independent of temperature. For our high resistivity, undoped In_2O_3 layers prepared with decreasing substrate temperature T_2 to about 410°C (cf. Figure 2 of the preceding article (1)) to obtain $n \sim 4\text{-}5.10^{19}$ cm^{-3} we observed a slight dependence of the mobility $\mu_H \sim T^{0.5-1}$, as in the case of undoped SnO_2 layers. For a non-degenerate electron gas $\mu_H \sim T^{3/2}$ when impurity scattering is the predominant mechanism, the lower temperature dependence of μ_H can be ascribed to the fact that the electron gas is still degenerate. It is interesting to note that the increase of resistivity corresponding to a decrease of the substrate temperature T_2 (cf. Figure 2 of the preceding article (1)) should be attributed to both a decrease in n and μ_H. These observations have been made by Caroll and Slack (3) and Muller (4) as well, and correspond to a decrease in crystallinity as has been pointed out.

Heat treatment:

When heating SnO_2 : F or In_2O_3 : Sn layers, some irreversible changes will occur if the annealing temperature T is high enough; T will depend upon the preparation conditions for the layers. We did not use temperatures higher than 500°C, for the coatings deteriorate (7, 8) when heated above these temperatures, due to the diffusion of alkali from the substrate into SnO_2 or In_2O_3 layers. Results are reported in Table 2.

Undoped In_2O_3 and SnO_2 layers: for these layers, the stoichiometric deviation is known to be important (9, 10, 11). Heating in oxidizing ambient lead to an increase

TABLE 2

Variation in the sheet resistance $R_\square$ following annealing in air or in argon.

Successive heat treatment	SnO_2 undoped	In_2O_3 undoped	SnO_2 : F	In_2O_3 : Sn
Initial value $R_\square$	110	250	10	10
Annealing (1) in Ar 1 hour T = 400°C	90	200	10	7
Annealing (2) in air 1 hour T = 400°C	140	450	10	11.5
Annealing (3) in Ar 1 hour T = 400°C	90	200	10	7
Annealing (4) in Ar 1 hour T = 400°C	90	200	10	7

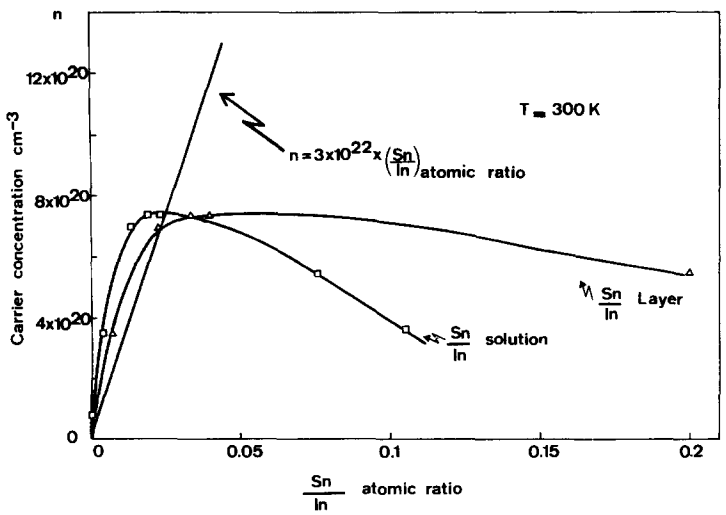

FIG. 2

Free electron density versus Sn/In atomic ratio -- In_2O_3 : Sn layers. The dotted line is the theoretical free electron concentration, assuming each Sn ion sponsor one electron.

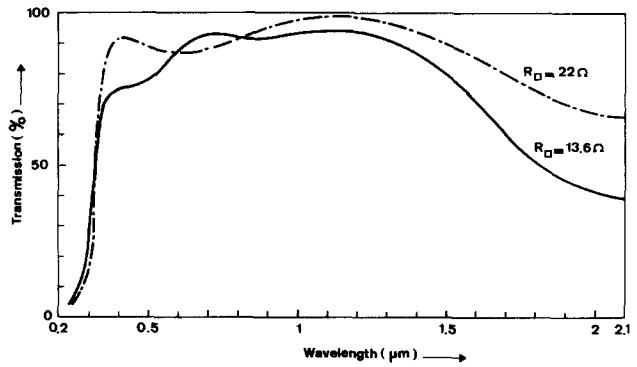

FIG. 3

Transmission spectra for two In_2O_3 : Sn layers having different sheet resistance.

of the resistivity (3, 12). This is attributed to an oxidation of the films removing oxygen vacancies; the chlorine ions accounting for the high remnant n-type conduction (cf. Table 2). Heating under vacuum or inert ambient leads to a decrease in resistivity corresponding to an increase in the carrier concentration. These annealing cycles are reversible: after a heat treatment under vacuum, the properties without annealing can be restored (4) by heating the samples in air (cf. Table 2).

In highly doped SnO_2 : F layers no variation was noted for the resistivity for heat treatment in air or inert ambient: Ar. In this case, the carrier concentration is due to the presence of dopant fluorine in substitution with oxygen. This was noted in an unambiguous way by Kane and Schweitzer (7) who observed that SnO_2 : Sb samples prepared on sapphire substrate show no change in the sheet resistance after being heated several hours to 1000°C.

In the case of highly doped In_2O_3 : Sn layers both the contribution to the conductivity of the ionized donors (tin) and the stoichiometry deviation must be taken into account. This is shown in Figure 2, where the carrier concentration is reported versus Sn/In atomic ratio. If we assume that every quadrivalent Sn^{++++} cation substitutes a trivalent In^{+++} cation in the In_2O_3 lattice and sponsors one free electron to the conduction band, then the experimental n(Sn/In) curve should follow a straight line. This is not the case, the experimentally determined n values being higher than this linear law:

$$n\ (cm^{-3}) = 3.10^{22} \cdot \left(\frac{Sn}{In}\right)\text{atomic ratio}$$

determined assuming for In_2O_3 a specific density of 7 g cm^{-3} (13). We must conclude that other contributions to the free electron density arise from stoichiometric deviation (oxygen vacancies) or chlorine impurity substitutionally incorporated at an oxygen site. Of course, this analysis is valid at low Sn concentration; for higher concentration both the decrease in crystallinity and the compensation of donor action for the tin atoms explain the decrease of the carrier concentration.

The heat treatment results are in good accordance with this analysis. After annealing under inert ambient (Ar), a decrease in the sheet resistance is observed even for highly doped samples (cf. Table 2) corresponding to the creation of oxygen vacancies. This is also explained (14) in the case of In_2O_3 : Sn layers prepared using a reactive sputtering method by a dissociation of SnO and the incorporation of Sn in the In_2O_3 lattice. This should not be the case for our samples because of the reversibility of the sheet resistance variation (cf. Table 2) for annealing under Ar or in air, and vice versa.

The increase in R after a heat treatment in air is relatively more important for thinner samples. This is in good accordance with the observations of Bosnell and Waghorne (15) and Vassen (16) who note that for thick films a passivating surface oxide is grown on the film surface, preventing deeper oxidation. The influence of the stoichiometric deviation in the carrier concentration of In_2O_3 : Sn samples is shown unambiguously according to the subsequent experiment. Double layers of glass substrate - In_2O_3 : Sn - SnO_2 : F and glass substrate - SnO_2 : F - In_2O_3: Sn have been made. Each In_2O_3 : Sn and SnO_2 : F thin film having approximately the same sheet resistance $R_\square = 10\,\Omega$. In the former case, a heat treatment of many hours under Ar or in air did not show any variation of the sheet resistance of the layers. As we already know that the SnO_2 : F is stable for such a treatment, we must conclude that this layer prevents any stoichiometric deviation for the In_2O_3 : Sn underlying film. In the second case we did observe a modification of the sheet resistance corresponding to a modification in the In_2O_3 : Sn layer in contact with the ambient.

Optical Properties

The optical properties were studied by measuring the transmission T between $\lambda = 0.25\ \mu m$ and $\lambda = 3\ \mu m$, and the reflection R between $\lambda = 2.5\ \mu m$ and $\lambda = 50\ \mu m$.

Visible and near infra-red regions:

Transmission spectra for two typical In_2O_3 : Sn layers are given in Figure 3. In the transparent region of these layers, the variations of transmission are due principally to interference phenomena. The films exhibit transmission averaging 85 - 90% between $\lambda = 0.4$ and 1.5 μm for sheet resistivities greater than $10\,\Omega_\square$. Similar transmission spectra are obtained for SnO_2 layers (8, 9). The refractive index for the In_2O_3 : Sn and SnO_2 : F layers have been determined versus the wavelength for the thicker films according to the method developed elsewhere (9, 17) for SnO_2 films. It is then assumed that this value found for the index of refraction is independent of the thickness of the layer (other fabrication parameters being equal) and can be used for the evaluation of the thicknesses of thinner films. It should be noted, however, that there is an important scattering between the values determined for the refractive indexes amongst different authors (4, 5, 18, 19, 20).

Kane and Schweitzer (18) observed an important scattering for n between 1.66

and 2.48 at λ = 0.55 μm for In_2O_3 : Sn films prepared using a C.V.D. method. They found also (7) that the presence of H_2O in the films leads to a decrease for the refractive index. Spray or sputtering methods of fabrication lead to more reproducible n values. For In_2O_3 : Sn layers having the best overall characteristics (higher transparency and lower resistivity) values for n range between 1.9 and 1.97 in the visible and near infra-red. Using spray or sputtering techniques (4, 5, 20), slightly higher values for n = 1.97 - 2 are reported for a wavelength λ = 0.45 - 0.5 μm. For SnO_2 and SnO_2 : F spray layers n values range between 1.87 and 1.92 (9, 10, 12). For some layers we used a Talystep apparatus to evaluate the thicknesses, both methods giving similar results.

U.V. region:

For SnO_2 or In_2O_3 layers, the absorption edge is strongly dependant on the method of preparation (9). Usually for In_2O_3 and SnO_2 thin films optical gap is found around 3.5 - 3.8 eV. Baillou et al. (21) report a value as low as 3.1 eV for the absorption edge of SnO_2 prepared using a reactive sputtering method. In the fundamental absorption region, the transmission is given by:

$$T = A \exp\left(\frac{-4\pi kt}{\lambda}\right) \quad (1)$$

k being the extinction coefficient and t the thickness of the film. For $k^2 \ll n^2$, the principal variation of T occurs in the exponential term with A not too different from unity (9).

$$T \sim \exp(-Kt) \quad (2)$$

and for the absorption coefficient $K = \frac{4\pi k}{\lambda}$.

The variation of the absorption coefficient K with the energy of the incident light is shown in Figure 4 for In_2O_3 : Sn samples having different carrier concentrations. We observed that the higher the free electron density, the shorter the wavelength of

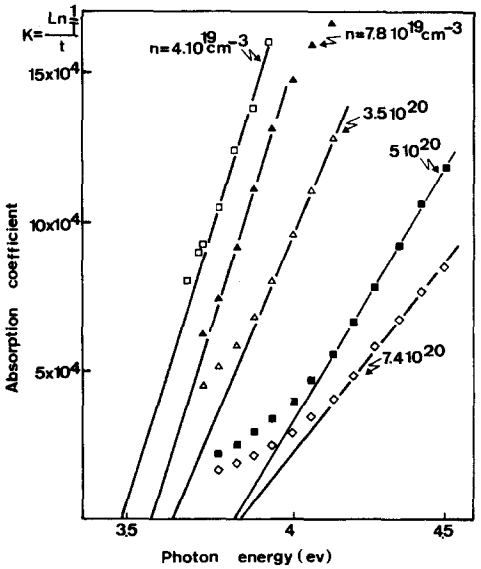

FIG. 4

Variation of the absorption coefficient K versus photon energy - In_2O_3 : Sn layers having different carrier concentrations.

intrinsic absorption edge (6, 9, 22). A very simple analysis could explain this phenomenon when the density of free electrons is so high that the conduction band is partially filled up, then the first transition observable occurs for higher photon energy. This shift ΔE can be described (23) assuming a Fermi free electron gas relating:

$$\Delta E = E_F - E_c = \frac{h^2}{2m_{v_c}} (3\pi^2 n)^{2/3} \qquad (3)$$

where E_c is the bottom of the conduction band, n the free carrier density and m_{v_c} is a conduction band electron mass being affected here by the valence band curvature (22). This is shown in Figure 5, where the $n^{2/3}$ law (cf. equation (3)) is approximately followed. The value of m_{v_c} can be deduced: we found $m_{v_c} \approx 0.7\ m_e$. The same analysis can be carried out for SnO_2 : F samples; the absorption edge is found between 3.65 and 3.85 eV.

I.R. region:

Reflection data for an In_2O_3 : Sn layer and for the borosilicate substrate are shown between $\lambda = 2.5\ \mu m$ and $\lambda = 50\ \mu m$ in Figure 6. The important reflection observed is due to the high concentration of free electrons, none of the characteristics of the underlying pyrex substrate being detected. No absorption bands were detected in the I.R. spectra for In_2O_3 : Sn as reported for SnO_2 or SnO_2 : Sb films (6, 7, 12, 19).

Discussion

Origin of the n-type conduction:

The n-type conduction of these oxides depends on two different mechanisms: (1) a stoichiometric deviation and (2) a doping effect of some impurities (for example, Cl^- ions in the case where no doping agent has been intentionally added to the spraying solution). Both these mechanisms added to the various methods of preparation explain the disparity, according to different authors, found in the electrical properties of these layers. Vincent (11) applied the analysis given by Verwey (24), describing the basic difference between nonstoichiometric and controlled valence semiconductors, to

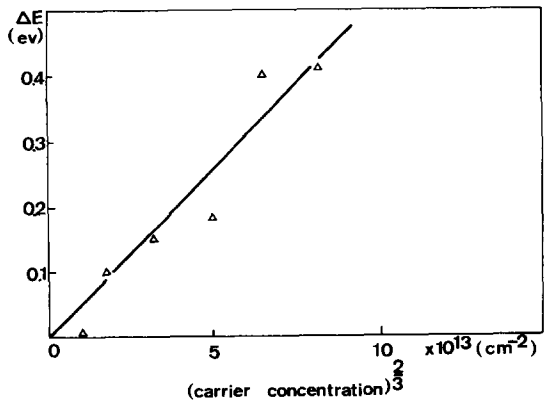

FIG. 5

Shift ΔE of the U.V. absorption edge versus the free electron density - In_2O_3 : Sn layers.

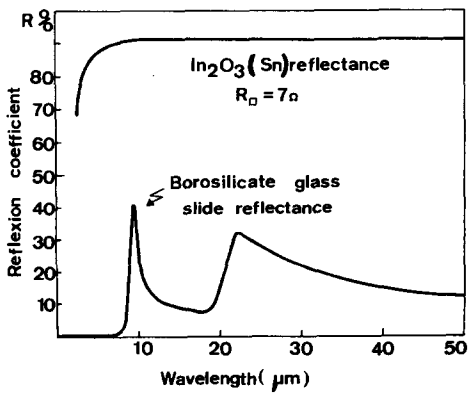

FIG. 6

Reflection spectra for an In_2O_3 : Sn layer and for a borosilicate glass slide.

the case of polycristalline tine oxide films. In the nonstoichiometric semiconductors, for every ion of deviating valency inserted into the lattice, a defect such as a lattice vacancy must also be introduced; in the controlled valence semiconductors, impurity ions are added without incorporation of lattice defects. This analysis can be applied to the case of doped or undoped SnO_2 and In_2O_3 layers.

Undoped SnO_2 and In_2O_3 layers:

SnO_2 and In_2O_3 in crystalline form are insulators. The high n-type conductivity observed for the polycrystalline thin films can be explained by two distinct phenomena:

1. the creation of defects: usually oxygen vacancy. For example, on combining x moles of SnO with (1-x) moles of SnO_2, we obtain the nonstoichiometric oxide:

$$Sn^{4+}_{(1-x)} \; Sn^{2-}_{x} \; O^{2-}_{(2-x)}$$

It contains x moles of oxygen atom vacancies, and the xSn^{2+} ions can donate 2x moles of electrons for conduction.

2. the presence of impurities: in the case of tin oxide films prepared by pyrolisis of tin chlorides, the conductivity is due in part to the inclusion of chloride ions in the lattice. We then have the controlled valence semiconductor:

$$Sn^{4+} \; e_x \; O^{2-}_{(2-x)} \; Cl^{-}$$

It has no defect, the structure still being cassiterite. In the case of undoped In_2O_3 layers, the same analysis applies: vacancies and/or substitutional (Cl^-) impurities can act as donors in the anion sub lattice. In this case anyway, another type of defect, intersticial In^{3+} cations, seems to be important (13), structural consideration being not in contradiction with intersticial indium.

The annealing experiment (cf. Table 2) shows that both these phenomena (substitutional impurities and oxygen vacancies) are important for the conduction properties of SnO_2 and In_2O_3 layers. The reversibility observed in the sheet resistance value for alternating heat treatment under inert and oxidizing ambient is explained as follows: annealing in air leads to a decrease in the stoichiometric deviation (corresponding to a decrease for oxygen vacancies) and so to an increase in resistivity and vice versa. The remnant n-type conductivity after prolonged oxidation is accounted for by impurity chlorine ions.

SnO_2 : F layers:

Addition of a group V element Sb, P, . . . in substitution for Sn cause the resistivity to decrease (as the addition of a group III element In, Al, . . . causes it to increase). In the same manner, addition of a group VII element, fluorine, in substitution for oxygen causes an important decrease in resistivity. This doping effect is due to a controlled valence mechanism. SnO_2 : F and SnO_2 : Sb are controlled valence oxides:

$$Sn^{4+} \; e_x \; O^{2-}_{(2-x)} \; F^{-}_{x} \quad \text{and} \quad Sn^{4+}_{(1-x)} \; Sb^{5+}_{x} \; e_x \; O^{2-}_{2}$$

Here the contribution of oxygen vacancies to the n-type conduction is negligible, as

annealing in any ambient does not modify the resistivity (cf. Table 2) (3, 6, 7).

In_2O_3 : Sn layers:

For these layers, we have a substitutional alloy oxide with oxygen vacancies still playing an important role. This can be seen in Table 2 where even for highly conductive In_2O_3 : Sn films, annealing has an important effect on resistivity. Vassen (16) and Bosnell and Waghorne (15) observed that the lowest resistivities In_2O_3 : Sn layers were obtained by sputtering in pure argon, leading to the creation of anion vacancies. In addition to donor doping by tin, Fraser and Cook (20) using a similar method found that the resistivity of the film was more sensitive to oxygen vacancy than it was to the tin content. In the case of In_2O_3 : Sn films, we will have both the controlled valence semiconductor

$$In^{3+}_{(2-x)}\ Sn^{4+}_{x}\ e_x\ O^{2-}_{3}$$

and the non-stoichiometric semiconductor

$$In^{3+}_{2}\ O^{2-}_{(3-x)}\ e_{2x}$$

However, matters are not so simple in the case of In_2O_3 : Sn layers. Bosnell and Waghorne (15) note that an intermediate tin oxide state must be present in the mixed oxide films, consistent with Sn_3O_4, the possibility of compound formation of $In_xSn_yO_3$ being less likely.

To finish we should note that all the consequences of the loss of crystallinity for high doping was neglected. It can be seen from Figures 1 and 2 of the preceding article (1) that the trend predicted by the controlled valency mechanism is reversed, due to an increase of molecular disorder, for large additions of Sn (In_2O_3) or F (SnO_2). The differences in crystalline quality according to the various methods of preparation could easily explain the scattering in the Sn/In atomic ratio found to give the lower resistivity films. We found an atomic ratio Sn/In = 0.04 as for Kane and Schweitzer (18) using a C.V.D. method, different from the results of Fraser and Cook who found a ratio Sn/In = 0.2 to give the best results.

Application to solar energy conversion - solar cell technology:

These transparent electrodes must have two contradictory characteristics: they must be transparent and, so, thin, yet conductive and, so, thick. Haacke (25) defined a figure of merit for transparent conductors

$$\phi_{TC} = \frac{T^{10}}{R_{\square}} \qquad (4)$$

We reported for comparison in Table 3 characteristic parameters and values of ϕ_{TC} for various conductive and transparent layers. It is interesting to note that ϕ_{TC} for layers obtained using a spray method is better than that of specimens prepared by other methods, showing the advantage of not using too conductive a deposit since this has a limiting effect due to its high carrier absorption. Moreover, from transmission and reflection spectra in the visible and near infra-red, it can be shown that the light absorption is negligible in this wavelength region. Anit-reflection coatings with transmission over 95% and sheet resistance under 10 $\Omega_{\square}$ thus appears possible. It should be borne in mind, that optimization parameters of the layers in the case of borosilicate glass slides could be different from those of silicon substrates in a Si-In_2O_3 : Sn solar

Authors	Deposits	$R_\square$ (Ω)	Transmission			ϕ_{TC} (10^{-3} . Ω^{-1})		
			λ =0.55μm	λ =0.9μm	λ =1.1μm	λ=0.55μm	λ =0.9μm	λ = 1.1μm
Fraser et al. (20)	In_2O_3/SnO_2 (sputtering)	3.1	0.83	0.77	0.64	50	24	3.7
Haacke (28)	Cd_2SnO_4 (sputtering)	2.4	0.84	0.82	0.7	73	57	11.8
Our results	In_2O_3 (Sn) (spray)	9	0.85	0.92	0.92	22	48	48
	SnO_2 (F) (spray)	10.6	0.85	0.88	0.86	18.5	26	21
Kane et al. (7)	SnO_2 :Sb (C.V.D.)	72	0.87			3.5		
Kane et al. (18)	In_2O_3 : Sn C.V.D.	3	0.75			19		

TABLE 3

Comparison of the figure of merit $O_{TC} = \frac{T^{10}}{R}$ for different transparent and conductive layers.

cell structure. As there is no problem of contamination by alkali ions, the substrate temperature T_2 could be increased over 500°C to lower the resistivity and thus the sheet resistance of the layers. A second important parameter is the barrier height ϕ_B of the Schottky diode. ϕ_B depends upon the electronic affinities of the semiconductor substrate and on the transparent electrode, as well as interface states. The higher ϕ_B, the higher the open-circuit voltage V_{oc} of the solar cell. Experimental results (26, 27) show that using a spraying method, V_{oc} for a Si (n) - SnO_2 : F structure was around 300 - 350 mV under AM1 condition. In the case of Si(n) = In_2O_3 : Sn structure V_{oc} as high as 500 mV have been obtained.

Application to solar energy conversion - flat plate collector technology:

These layers, especially SnO_2 : F layers which will be much less expensive than In_2O_3 : Sn layers, could be used as spectral selective windows having transmission over 90% in the solar spectrum (cf. Figure 3) and high reflectivity over 90% for thermal I.R. (cf. Figure 6). More generally, compared to other methods, the spraying method is easy to handle, cheaper, and can easily be connected on an industrial basis, where high production rates are necessary.

Conclusion

We have studied SnO_2 : F and In_2O_3 : Sn layers prepared using a very simple and cheap "spray" method. Most of the experimental work was done on layers prepared on borosilicate glass slides. These layers have an excellent adherence and stability, and sheet resistance lower than 10 $\Omega_\square$ can easily be obtained having transparency higher than 80 - 85% in the visible and near I.R. spectrum. By optimizing the thickness,

the transparent SnO_2 : F or In_2O_3 : Sn electrode can act as an efficient anti-reflection coating in heterojunction or Metal-Isolant-Semiconductor (M.I.S.) solar cell structures (as does SiO ir TiO_x in conventional structures). Combined with the high reflectivity, over 90% in the thermal infra-red, these films could be used in flat plate collector technology as spectral selective windows.

Acknowledgments

The authors would like to thank Professors M. Savelli, J. P. Fillard and P. Siffert for their support.

References

1. J.-C. Manifacier, L. Szepessy, J. F. Bresse, M. Perotin and R. Stuck, Mat. Res. Bull. 13, 109 (1978).
2. F. Van der Maesen and C. H. Witmer, Comptes Rendus du 7^{o} Congrès International, Physique des Semiconducteurs, DUNOD, 1211, Paris (1964).
3. A. F. Carrol and L. H. Slack, J. Electrochem Soc. 123, 1889 (1976).
4. H. K. Müller, Phys. Stat. Sol. 27, 723 (1968).
5. R. Groth, Phys. Stat. Sol. 14, 69 (1966).
6. T. Arai, J. Phys. Soc. Jap. 15, 916 (1960).
7. J. Kane and H. P. Sweitzer, Thin Solid Films 29, 155 (1975).
8. J.-C. Manifacier, M. De Murcia and J. P. Fillard, Mat. Res. Bull. 10, 1215 (1975).
9. J.-C. Manifacier, M. De Murcia and J. P. Fillard, Thin Solid Films 41, 127 (1977).
10. K. Ishiguro, T. Sasaki, T. Arai and I. Imai, J. Phys. Soc. Jap. 13, 296 (1958).
11. C. A. Vincent, J. Electrochem. Soc. 119, 515 (1972).
12. V. K. Miloslavskii, Optics and Spectroscopy 7, 154 (1959).
13. J. H. W. Dewit, J. Sol. State Chem. 8, 142 (1973).
14. F. Buigez, G. Bromchill, S. Galzin and A. Monfret, Colloque Microélectronique, 146, Montpellier, France 16-19 Nov. (1976).
15. J. R. Bosnell and R. Waghorne, Thin Solid Films 15, 141 (1973).
16. J. L. Vossen, RCA Rev. 32, 289 (1971).
17. J.-C. Manifacier, J. Gasiot and J. P. Fillard, J. Phys. E. 9, 1002 (1976).
18. J. Kane and H. P. Schweitzer, Thin Solid Films 29, 155 (1975).
19. J. Kane, H. P. Schweitzer and W. Kern, J. Electrochem. Soc. 123, 270 (1976).
20. D. B. Fraser and H. D. Cook, J. Electrochem. Soc. 119, 1368 (1972).
21. J. Baillou, P. Pugnet, J. Deforges, S. Durand and G. Batailler, Rev. Phys. Appl. 3, 78 (1968).
22. H. Köstlin, R. Jost and W. Lems, Phys. Stat. Sol. (a) 29, 87 (1975).

23. C. Kittel, Introduction to Solid State Physics, Third Edition, p. 208. John Wiley Sons, New York (1968).

24. E. J. W. Verwey, Semiconducting Materials, H. K. Henisch, Editor. Butterworth, London (1951).

25. G. Haacke, J. Appl. Phys. 47, 4086 (1976).

26. J.-C. Manifacier and L. Szepessy, Appl. Phys. Lett. 31, 459 (1977).

27. M. Perotin, L. Szepessy, J.-C. Manifacier, P. Parot, J. P. Fillard and M. Savelli, Colloque International sur l'Electricite Solaire, p. 481, Toulouse, France, 1-5 March (1976).

28. G. Kaacke, Appl. Phys. Lett. 28, 622 (1976).